Protein Science (2000), *9*:1439–1454. Cambridge University Press. Printed in the USA.

Blue copper proteins: A comparative analysis of their molecular interaction properties

F. DE RIENZO,[1,2] R.R. GABDOULLINE,[1,3] M.C. MENZIANI,[2] AND R.C. WADE[1]

[1]European Molecular Biology Laboratory, Postfach 10 2209, Meyerhofstrasse 1, 69012 Heidelberg, Germany
[2]Universita' degli studi di Modena e Reggio Emilia, Dipartimento di Chimica, Via Campi 183, 41100 Modena, Italy
[3]Institute of Mathematical Problems in Biology, RAS, Pushchino, Moscow Region 142292, Russia

(RECEIVED December 13, 1999; FINAL REVISION May 5, 2000; ACCEPTED May 25, 2000)

Abstract

Blue copper proteins are type-I copper-containing redox proteins whose role is to shuttle electrons from an electron donor to an electron acceptor in bacteria and plants. A large amount of experimental data is available on blue copper proteins; however, their functional characterization is hindered by the complexity of redox processes in biological systems. We describe here the application of a semiquantitative method based on a comparative analysis of molecular interaction fields to gain insights into the recognition properties of blue copper proteins. Molecular electrostatic and hydrophobic potentials were computed and compared for a set of 33 experimentally-determined structures of proteins from seven blue copper subfamilies, and the results were quantified by means of similarity indices. The analysis provides a classification of the blue copper proteins and shows that (1) comparison of the molecular electrostatic potentials provides useful information complementary to that highlighted by sequence analysis; (2) similarities in recognition properties can be detected for proteins belonging to different subfamilies, such as amicyanins and pseudoazurins, that may be isofunctional proteins; (3) dissimilarities in interaction properties, consistent with experimentally different binding specificities, may be observed between proteins belonging to the same subfamily, such as cyanobacterial and eukaryotic plastocyanins; (4) proteins with low sequence identity, such as azurins and pseudoazurins, can have sufficient similarity to bind to similar electron donors and acceptors while having different binding specificity profiles.

Keywords: blue copper proteins; electrostatic potential; electron transfer; hydrophobic potential; protein–protein interactions; redox proteins; similarity index

Blue copper proteins, which are also known as cupredoxins, are small, soluble proteins (10–14 kDa) whose active site contains a type-I copper. As far as it is known, they exert their function by shuttling electrons from a protein acting as an electron donor to another acting as an electron acceptor in various biological systems, such as bacterial and plant photosynthesis (Baker, 1994; Sykes, 1994).

A large amount of structural and spectroscopic data is available for the blue copper proteins, which have been named and classified into subfamilies according to their spectroscopic properties (Adman, 1991). High resolution X-ray and NMR structures are known for several members of each of the plastocyanin, azurin, pseudoazurin, and amicyanin subfamilies (Baker, 1994), and for single members of three further subfamilies, the rusticyanins (Harvey et al., 1998), the cucumber basic proteins (CBP) (Guss et al., 1996), and the stellacyanins (Hart et al., 1996). Despite often showing low (<20%) sequence identity, all these proteins possess an eight-stranded Greek key β-barrel or β-sandwich fold and have a highly conserved active site architecture (Baker, 1994; Sykes, 1994). Important information concerning the functional role and the binding properties of the cupredoxins is provided by the two available experimental structures of cupredoxin protein complexes: an X-ray structure of amicyanin from *Paracoccus denitrificans* interacting with both its electron donor, methylamine dehydrogenase (MADH), and its electron acceptor, cytochrome c551i (Chen et al., 1994); and an NMR-based structure of the complex of plastocyanin from *Spinacia oleracea* (spinach) and its electron donor, cytochrome f from *Brassica rapa* (turnip) (Ubbink et al., 1998).

Many experimental data are available for blue copper proteins from mutagenesis studies, kinetic analysis, and biochemical assays (Gross et al., 1990; van de Kamp et al., 1990; Qin & Kostic, 1993; Baker, 1994; Sykes, 1994; Ubbink et al., 1994; Van Pouderoyen et al., 1994; Kukimoto et al., 1995, 1996; Lee et al., 1995; Yamanaka & Fukumori, 1995; Hibino et al., 1996; Libeu et al., 1997; Sigfridsson et al., 1997; Young et al., 1997). Some of these data are contradictory and, due to the complexity of the molecular recognition processes associated with redox systems, a full interpretation and explanation of these data has yet to be achieved.

Reprint requests to: Rebecca C. Wade, European Molecular Biology Laboratory, Postfach 10 2209, Meyerhofstrasse 1, 69012 Heidelberg, Germany; e-mail: wade@embl-heidelberg.de.

Plastocyanins are found in cyanobacteria, algae, and plants, where they play a role in the photosynthetic process by shuttling electrons from cytochrome f to photosystem I (PSI). Azurins and pseudoazurins participate in denitrification processes in bacteria. Amicyanins participate in the oxidizing electron transport chain of some methylotropic bacteria (Baker, 1994). The only known rusticyanin is thought to be fundamental in the iron respiratory chain of the bacterium *Thiobacillus ferrooxidans*, where it probably shuttles electrons from cytochrome c552 to cytochrome oxidase (Yamanaka & Fukumori, 1995; Harvey et al., 1998). CBPs and stellacyanins are plant-specific blue copper proteins belonging to a subgroup defined as phytocyanins (Nersissian et al., 1998). Knowledge about CBPs, also known as plantacyanins, and stellacyanins is very limited. CBPs are unglycosylated single domain proteins that are probably located in the endoplasmic reticulum, and stellacyanins are glycoproteins found in nonphotosynthetic plant tissue (Nersissian et al., 1998).

While the biological role of some of the cupredoxins has been established for most cupredoxins, either the electron donor or the electron acceptor is unknown. The difficulties in functional characterization of the blue copper proteins stem in part from the fact that, depending on their experimental growth conditions, organisms can express different types of proteins that are able to play the same or similar physiological roles. Thus, more than one donor or acceptor suitable for interaction with the same cupredoxin might exist and, at the same time, the cupredoxin itself might be substituted with other isofunctional proteins (Williams et al., 1995; Yamanaka & Fukumori, 1995; Ullmann et al., 1997a). This versatility, dubbed "pseudospecificity" (Williams et al., 1995), can be achieved by cupredoxins having binding faces of varying specificity but it is currently unclear to what extent the binding of blue copper proteins to their redox partners is specific and to what extent specific binding is important for electron transfer.

The aim of this work is to gain insights into the recognition properties of the blue copper proteins by comparative analysis of their interaction features. We focus on molecular electrostatic potentials, which are considered to be especially important in biological molecular recognition processes at medium and long range distances, and hydrophobic patches on the protein surfaces, which may be involved in short range docking and be important in electron transfer processes. All subfamilies for which experimental three-dimensional (3D) structures are available are analyzed.

Related approaches have been used in previous work to investigate the specificity of the docking processes in redox systems. Among others (Durell et al., 1990; Roberts et al., 1991; Pearson et al., 1996), Williams et al. (1995) compared the surface features of a pseudoazurin (from *Thiosphaera pantotropha*) with those shown by some of its known partners and by some isofunctional proteins and suggested that redox proteins could be involved in a pseudospecific docking mechanism. Ullmann et al. (1997a, 1997b) used the FAME alignment algorithm to compare the structural and electrostatic features of the physiologically isofunctional redox proteins, plastocyanin, and cytochrome c6 from *Chlamydomonas reinhardtii* and investigated the surface complementarity of plastocyanin and its electron donor cytochrome f.

To our knowledge, this paper is the first report of an extensive comparison of molecular recognition features applied to all the structurally characterized blue copper protein classes. The approach of using similarity indices to compare protein interaction properties that we adopt in this work has been applied previously to compare electrostatic potentials of other protein families (Demchuk et al., 1994; Wade et al., 1998; Blomberg et al., 1999). For the present analysis, molecular electrostatic and hydrophobic potentials were computed and compared for a set of proteins selected from the available experimentally-determined structures and representative of the different cupredoxin subfamilies. The results of the comparative analyses were quantified by means of similarity indices to obtain descriptors of the variability of the investigated molecular properties among the proteins. Sequence and structure analyses were also performed to relate the results obtained from the recognition property comparisons to sequence and structure information.

Results

Sequence and structure analysis

The sequence analysis was carried out using structure-based pairwise sequence alignments (Fig. 1). The use of structural information in the alignment procedure is particularly important for the blue copper protein family, since proteins belonging to different subfamilies share similar folds although they have low (sometimes $<20\%$) sequence identity. Computed pairwise sequence identity percentages are given in file 1.mat in Supplementary material in the Electronic Appendix. These were used to derive a sequence-based distance matrix to compare the proteins (see Materials and methods). A 3D projection of this can be viewed in Figure 2A and as a Kinemage in 1.kin of Supplementary material in the Electronic Appendix. This distribution shows that the different subfamilies are clustered in different regions of sequence space and every member of a subfamily is closer to its own subfamily cluster than to any other one.

All the plastocyanins, both eukaryotic and cyanobacterial, belong to the same cluster. The two amicyanins in the data set are clustered within the plastocyanin group, consistent with the known sequence and structural similarity between these two blue copper subfamilies (Van Beeumen et al., 1991) and their classification into the same class according to spectroscopic properties (Adman, 1991). Azurins and pseudoazurins fall into two well-separated clusters, reflecting the very low sequence identity between them (about 10%). Rusticyanin, stellacyanin, and CBP are, as expected, outliers.

Hydrophobic potential analysis

A hydrophobic area on the protein surface near the copper site is a common feature of the blue copper proteins (Baker, 1994). Since the copper site is thought to be the region where the electron transfer takes place, the presence of a hydrophobic patch in this area might be related to the specific biological role played by the cupredoxins as electron shuttles.

The analysis of the hydrophobic interaction fields of the blue copper proteins confirms that a conserved hydrophobic region is found only around the copper site. Therefore, further analysis was limited to this region. Automated clustering based on the distance matrix of similarity indices (listed in 2a.mat of Supplementary material in the Electronic Appendix) using the NMRCLUST program (Kelley et al., 1996) shows that the four pseudoazurins form a cluster separated from the other proteins. Visual inspection of the 3D projection of the distance matrix (see Fig. 2B and also 2.kin in Supplementary material in the Electronic Appendix) confirms this, showing the separate cluster of pseudoazurins. It also shows that

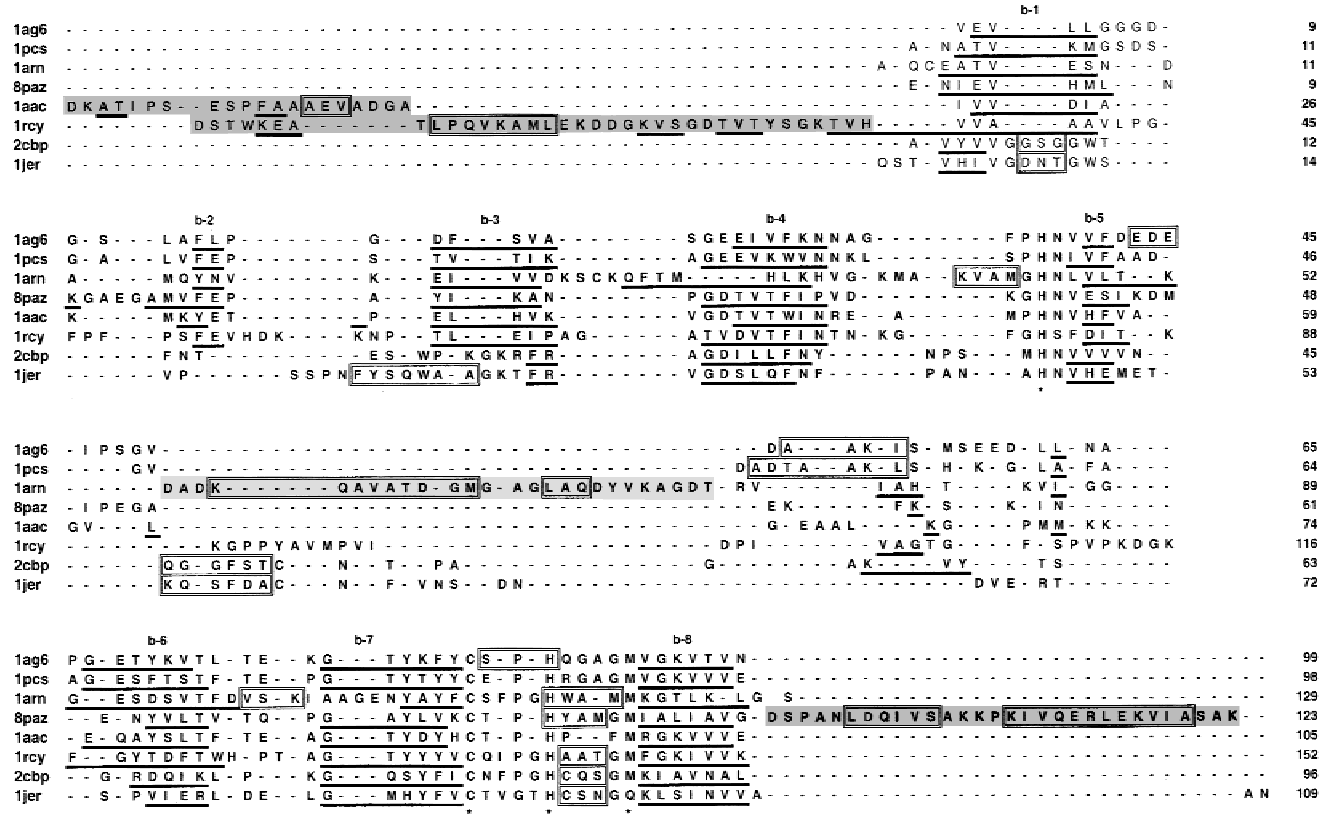

Fig. 1. Structure-based sequence alignment of eight blue copper proteins, representative of the seven subfamilies studied: plastocyanins (from eukaryota: 1ag6 and from cyanobacteria: 1pcs); azurins (1arn); pseudoazurins (8paz); amicyanins (1aac); rusticyanins (1rcy), CBP (2cbp), and stellacyanins (1jer). Black underlining indicates residues found in β-strands, while boxes indicate residues found in α-helices. β-Sheets are labeled using the lowercase letter/number pairs corresponding to the secondary structure of plastocyanin. Light gray shading indicates the back flap typical of azurin structures. Dark gray shading indicates additional segments in the N- or C-terminal regions. The asterisks indicate the Cu-ligand residues, whose atoms were used to optimize the structural superposition.

among the other proteins the amicyanins are clustered together with the azurins and the cyanobacterial plastocyanins; the eukaryotic plastocyanins are mostly grouped together and apart from these proteins; and stellacyanin and rusticyanin are outliers. A prominent hydrophobic patch, due to the presence of many long chain aliphatic residues, such as methionines and leucines, is present around the copper site in azurins, amicyanins, cyanobacterial plastocyanins, CBP, and, to a lesser extent, in pseudoazurins and eukaryotic plastocyanins. Hydrophobic patches are also present at the stellacyanin and rusticyanin copper sites, but they have different features. In rusticyanin, a large hydrophobic patch extends from the copper site to other regions on the protein surface. In stellacyanin, the patch is punctured by the two Cu-liganding histidines that protrude from the surface of the Cu-site. It is consequently more polar. It also contains mainly short chain aliphatic residues, so it is flatter than the hydrophobic patches on other cupredoxins.

Electrostatic potential analysis

Sensitivity to parameter variation

The method used to analyse the electrostatic potentials was tested to check its sensitivity to (1) the choice of the 3D structures to represent the proteins (see Materials and methods); and (2) the partial atomic charge parameter set used for the copper and its ligands. These tests showed that the method produces highly reliable and consistent results, as the choice of other appropriate structures or charge sets has negligible effects on the similarity index (SI) distributions. This has two important implications: (1) the choice of one specific protein conformation vs. another does not affect the results significantly; (2) it is possible to parameterize the copper and its ligands by means of a very simple and reproducible charge scheme (see Materials and methods).

On the other hand, the distribution of the SIs is sensitive to the redox state of the proteins, i.e., to the assignment of a formal charge of +1e (for the reduced state) or +2e (for the oxidized state) to the copper. The electrostatic potential in the region around the copper is clearly the most affected by changes in the copper oxidation state (see similarity index matrices and Kinemages 4A and 4B in Supplementary material in the Electronic Appendix). Such a correlation between the SI distributions and the formal charge on the copper should be considered an important property of the blue copper proteins. In fact, since the cupredoxins are redox proteins shuttling electrons between two other proteins, they should be able to interact with and bind different proteins in their different redox states. This suggests that the electrostatic features of the

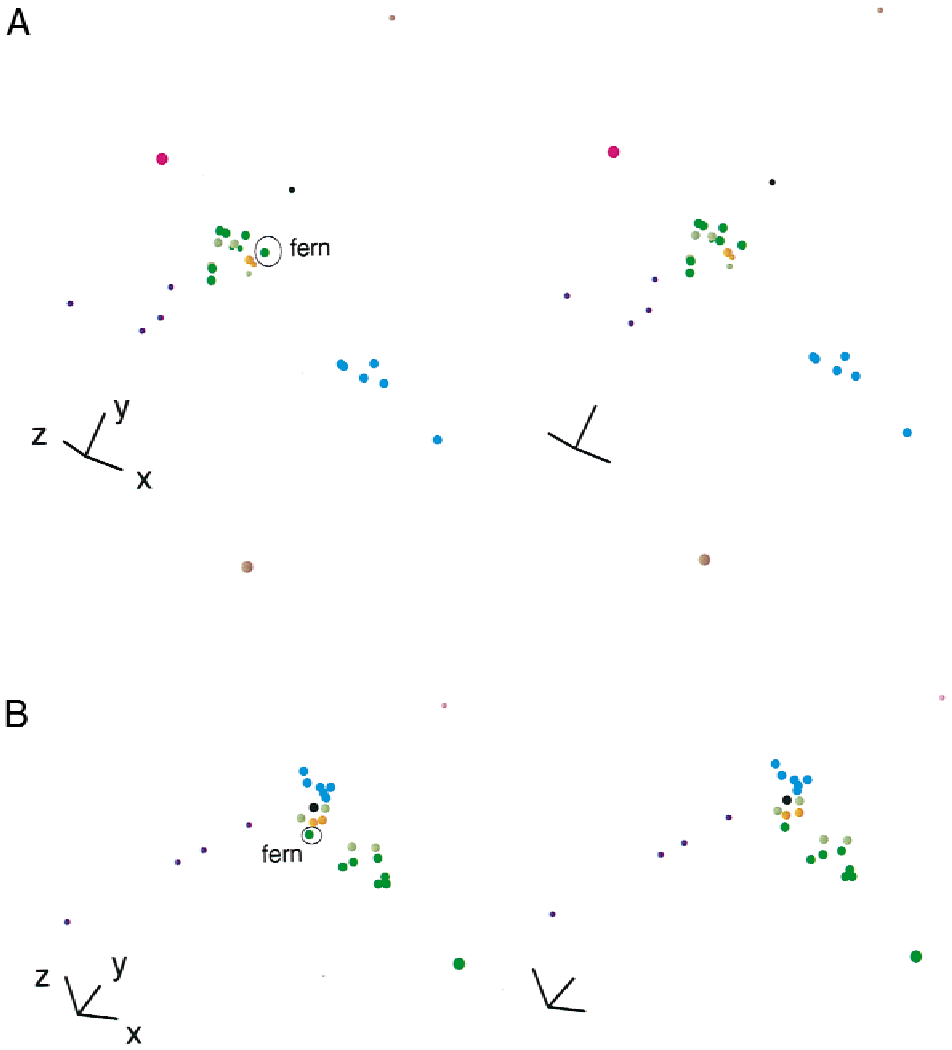

Fig. 2. Stereoview of the 3D distribution of (**A**) pairwise sequence identity percentages; (**B**) hydrophobic potential similarity indices, obtained from the analysis at the Cu site; (**C**) electrostatic potential similarity indices, calculated for the oxidized proteins at 0 mM; (**D**) electrostatic potential similarity indices, obtained from the analysis at the Cu-site and at 0 mM ionic strength of the oxidised proteins. Key: light green, cyanobacterial plastocyanins; dark green, eukaryotic plastocyanins; cyan, azurins; violet, pseudoazurins; orange, amicyanins; magenta, rusticyanin; black, CBP; brown, stellacyanin. The picture was generated with the Mage program. (*Figure continues on facing page.*)

reduced and oxidized proteins should be different, as highlighted by the spatial distribution of the electrostatic potential SIs in the copper site region.

The electrostatic potential analysis was carried out at two different ionic strengths, 0 and 150 mM, the latter value corresponding to the typical physiological ionic strength of biological systems. The overall trends and clustering of the proteins are generally conserved at the two ionic strengths, although they become more clearly apparent as the ionic strength is lowered (see Kinemages 3A, 3B), only the results obtained from the analyses at 0 mM are presented here. The greater simplicity of the SI distributions at 0 mM can be attributed to the different relative weights of higher order multipole terms at the two ionic strengths. At higher ionic strength, the relative contributions of the higher order multipole terms to the electrostatic potential are greater than at lower ionic strength values and, as a consequence, an increase in the sensitivity to protein local conformation is to be expected.

Analysis of SIs for different regions

The analysis of the molecular potential similarity was performed for different regions of the proteins. First, the electrostatic potentials of all the proteins were computed (Fig. 3); then the potentials were compared within the intersection of the complete skins of the proteins (Fig. 2C, similarity index matrices and Kinemages 3A and 3B in Supplementary material in the Electronic Appendix); finally, the potentials were compared in particular restricted regions that are expected to be important either for the binding or for the electron transfer processes (Fig. 2D, similarity index matrices and Kinemages 4A, 4B, 5A, and 5B in Supplementary material in the Electronic Appendix). These regions are indicated in Figure 4 and referred to as:

1. the “northern” site, around the copper site;
2. the “eastern” (or “remote”) site (around Tyr83 of plastocyanin from *Spinacia oleracea*);

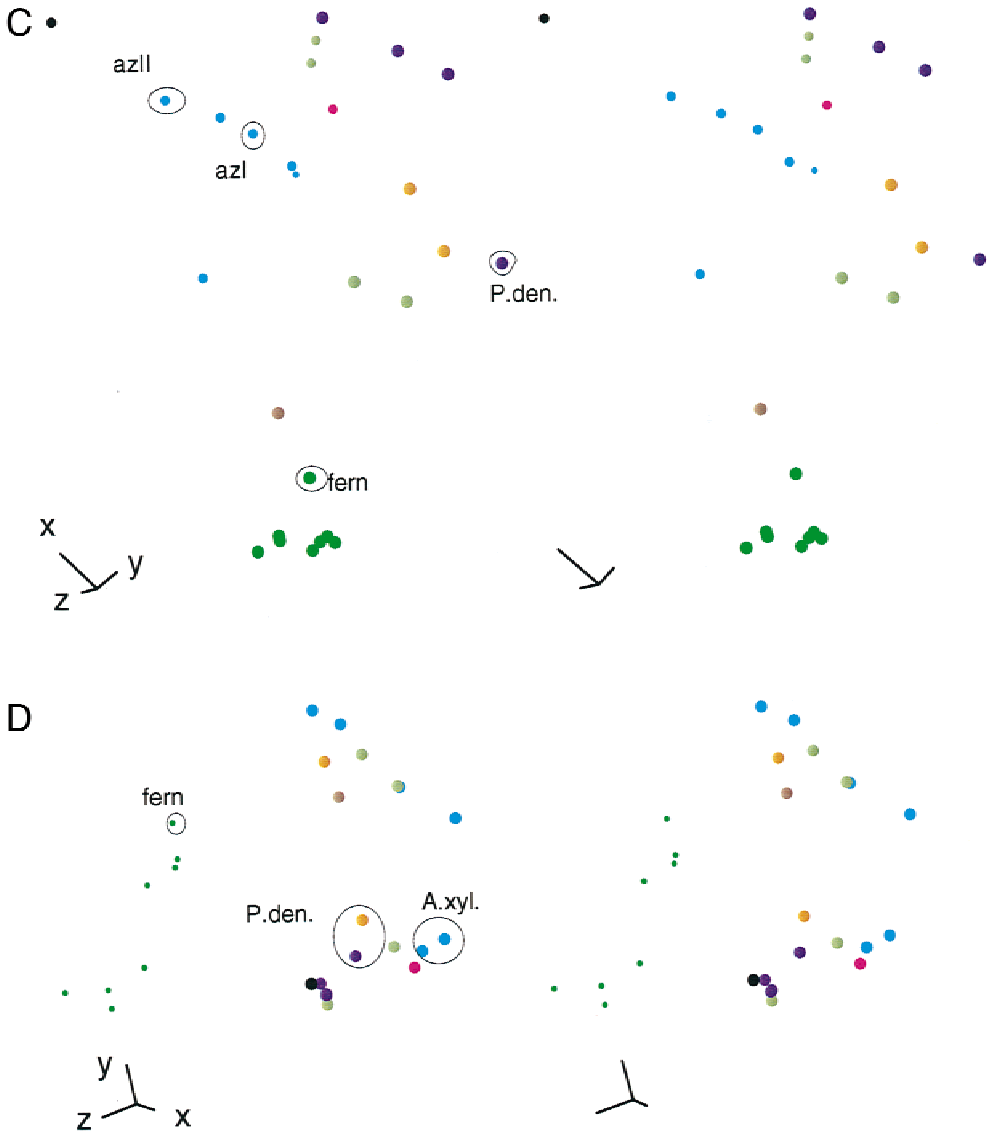

Fig. 2. *Continued.*

3. the "ami/cyt c551i" site (around Thr32 of amicyanin at the interface with cytochrome c551i in the crystal structure of the complex).

The molecular electrostatic potential around the copper site is important not only because this site is a likely electron transfer site but also because it has been suggested to act as the recognition site for the redox partners (van de Kamp et al., 1990; Baker, 1994; Kukimoto et al., 1995, 1996).

The "eastern" site is defined as the acidic region around a Tyr which is conserved in the plant plastocyanins. It is involved in binding cytochrome f in the NMR-based structure of the complex and is considered important for the recognition of both the electron donor (cytochrome f) and the electron acceptor (the PSI subunit containing the photosensitive chlorophyll P700+) proteins (Young et al., 1997). Moreover, the corresponding "eastern" region in amicyanin from *P. denitrificans* is involved in MADH binding in the crystal structure of the ternary complex. Interestingly, the "eastern" site, which lies between the fifth and sixth β-strands, is often referred to as "the variable region," since it is one of the less conserved regions in cupredoxins (Adman, 1991) (see Figs. 1, 4).

Investigation of the molecular potentials at the "ami/cyt c551i" site may reveal whether this region is important for molecular recognition processes in proteins other than the amicyanins.

The electrostatic potentials in the different regions were analyzed by clustering the proteins automatically on the basis of the full similarity distance matrices and by visual inspection of 3D projections of these distance matrices (see Fig. 2C,D and the matrices and Kinemages 3, 4, and 5 of Supplementary material in the Electronic Appendix). The clusterings obtained by these two analysis methods are consistent with each other. The results can be summarised by the following main points:

1. eukaryotic plastocyanins are clustered together and are separated from cyanobacterial plastocyanins and from all the other proteins;

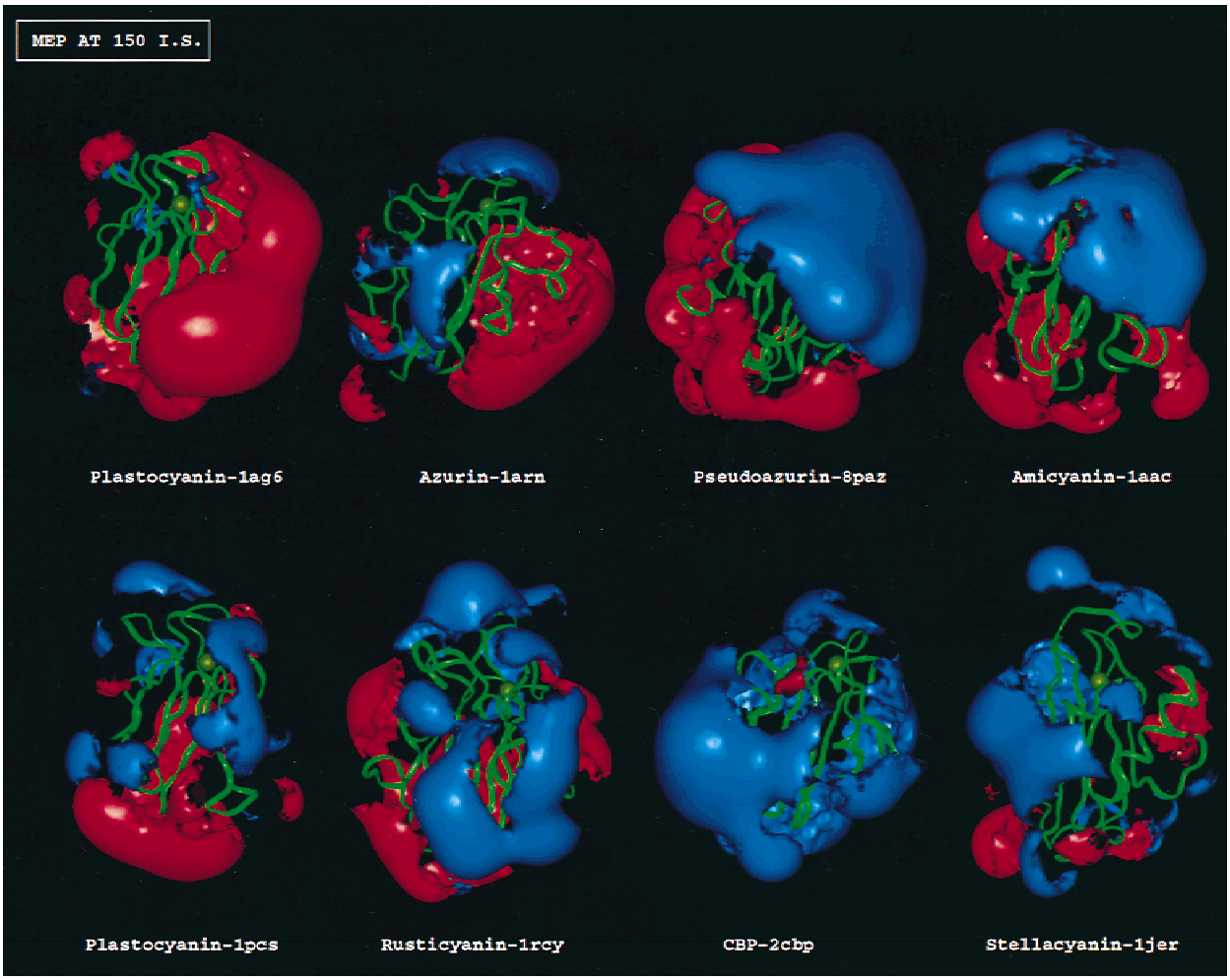

Fig. 3. Molecular electrostatic potentials (MEPs) computed at an ionic strength of 150 mM, for representative oxidized cupredoxins. The iso-potential contours are at −0.5 (red) and +0.5 kcal/mol/e (blue). The picture was generated with the InsightII program.

2. cyanobacterial plastocyanins generally belong to the same cluster as pseudoazurins and azurins;
3. the fern plastocyanin shows interaction features that are intermediate between those of the cyanobacterial and the eukaryotic plastocyanins;
4. azurins I and II from *Alcaligenes xylosoxidans* show similar electrostatic potential features at the copper site;
5. the pseudoazurins from *Alcaligenes faecalis* and *Achromobacter cycloclastes* have similar electrostatic potential features;
6. azurins I and II from *A. xylosoxidans* and pseudoazurins from *A. faecalis* and *A. cycloclastes* have electrostatic features that are similar in the region of the copper site, especially in their reduced forms;
7. amicyanins belong to the same cluster as the pseudoazurins rather than to plastocyanins, as for sequence-, structure-, and spectroscopic-based classifications (Adman, 1991). In particular, amicyanin from *P. denitrificans* is close to pseudoazurin from the *P. denitrificans* subspecies *T. pantotropha*;
8. rusticyanin appears somewhat similar to cyanobacterial plastocyanins and azurins;
9. CBP is an outlier with respect to its overall features, although around the Cu-site, it shows similarity to pseudoazurins;
10. stellacyanin is very similar to the fern plastocyanin when the overall molecular electrostatic potential distribution is considered, but in the zone around the Cu-site it shows close similarity to azurins.

Discussion

Sequence and structure comparisons for the blue copper proteins considered in this study were performed to provide a reference baseline from which to evaluate the 3D molecular interaction fields (MIFs). An important advantage of the approach used to evaluate the sequence similarity is that its results can be easily related to those from the MIF analyses, since both methods are based on pairwise protein comparison (see Fig. 2). We also computed the correlations between the pairwise sequence identity percentages and the pairwise MIF similarity indices (Fig. 5). Different trends

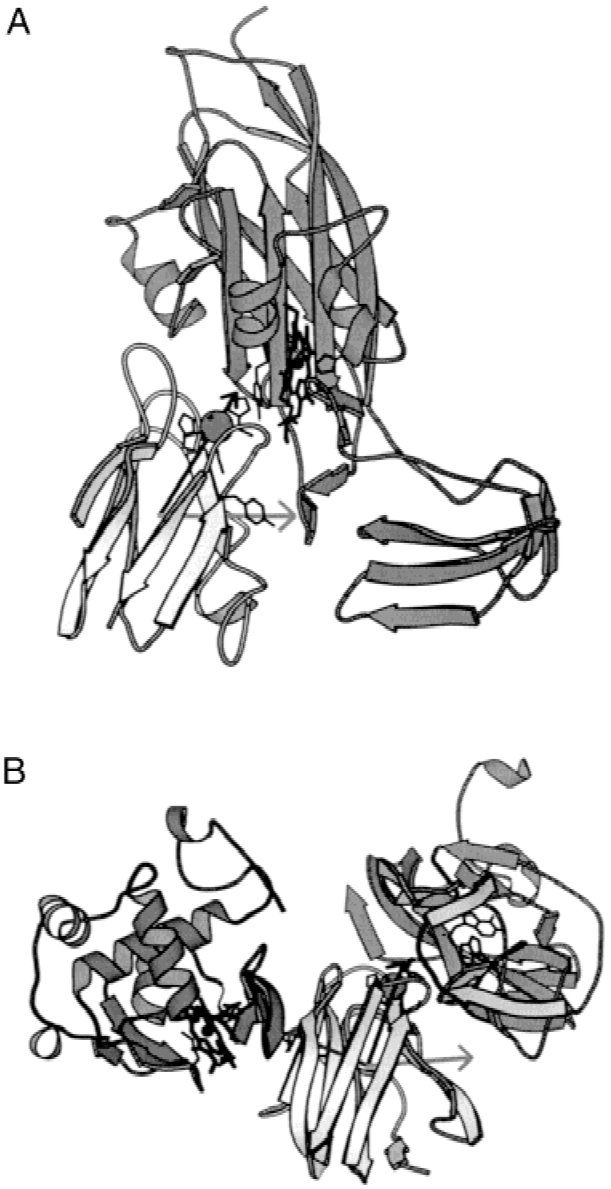

Fig. 4. A: The complex of plastocyanin from spinach and cytochrome f from turnip derived from NMR data. The arrows represent vectors from the center of mass of plastocyanin to the copper atom (black) and Tyr83, which is in the middle of the "eastern site" (light grey). **B:** The crystallographic complex of amicyanin with MADH and cytochrome c551i. The black and the light gray arrows are defined as in **A**; the dark gray arrow represents the vector connecting the center of mass of amicyanin to Thr32, which is in the middle of the "ami/cyt c551i" site. The pictures were generated with the MOLSCRIPT program (version 2.1).

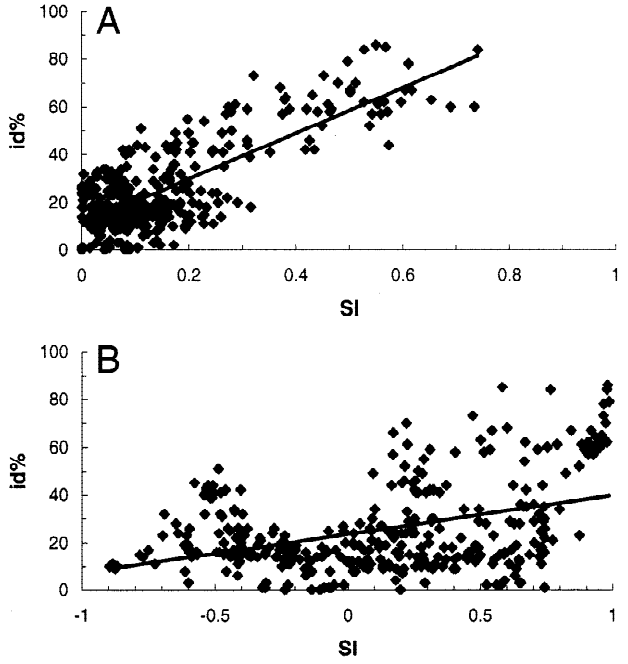

Fig. 5. A: Comparison between the cupredoxin pairwise sequence identity percentages (id%) and the hydrophobic potential similarity indices (SI). The linear regression is: id% = 94.93 SI + 10.90; $n = \sum_{i=1}^{26} i$; $r^2 = 0.61$; $r = 0.78$. **B:** Comparison between the cupredoxin pairwise sequence identity percentages (id%) and the electrostatic potential similarity indices (SI). The linear regression is: id% = 16.24 SI + 23.58; $n = \sum_{i=1}^{26} i$; $r^2 = 0.17$; $r = 0.41$.

are observed for the hydrophobic and the electrostatic properties of the proteins. Both the MIFs provide complementary information to sequence similarity although the hydrophobic MIF is more correlated with sequence identity than the electrostatic MIF.

Given the possible importance of hydrophobic features for the electron transfer process (Williams et al., 1995), it might be suggested that proteins belonging to the same subfamily should have similar electron transfer features. This rationale holds in part only, since the protein distribution in Figure 2B (and similarity index matrix and Kinemage 2 in Supplementary material in the Electronic Appendix) shows that eukaryotic and cyanobacterial plastocyanins, which share >40% sequence identity, have different hydrophobic properties.

The results of the MIF analysis are now discussed in the light of the structural and physiological information available for the different subfamilies.

Plastocyanin subfamily

At present, plastocyanins form the most well-characterized blue copper protein subfamily, with the greatest number of 3D structures from different organisms known (see Table 1). All the plastocyanins share the same fold, a flattened greek key β-barrel, which is also common to all other cupredoxins except the phytocyanins, and which is here referred to as the "plastocyanin-like" domain. The coordination of the copper is determined by the conformation of its three closest ligands, two histidine nitrogens and a cysteine sulfur, and of a fourth more distant ligand, a methionine sulfur (Redinbo et al., 1994). The role of plastocyanin is to shuttle electrons from cytochrome f to PSI in cyanobacteria, algae, and higher plants.

Eukaryotic and cyanobacterial plastocyanins: Different recognition properties

For electron transfer from eukaryotic plastocyanins to cytochromes f and PSIs, a mechanism consisting of two successive steps has been proposed (Sigfridsson et al., 1997; Ubbink et al.,

Table 1. *Structural and physiological information about the blue copper protein subfamilies*

Subfamily	Organism	Structural information: PDB code	State	Resolution (A)	Charge (e): Residue range	Ox	Red	E. Donor	E. Acceptor	References
Plastocyanin	Seed plant: *Spinacia oleracea*	1ag6	Ox	1.70	1–99	−7	−8			Xue et al. (1998)
	Seed plant: *Petroselinum crispum*	1plb	Ox	NMR	1–97	−6	−7			Bagby et al. (1994)
	Seed plant: *Populus nigra*	lpnd	Ox	1.60	1–99	−7				Guss et al. (1992)
		5pcy	Red	1.80	1–99		−8			Guss et al. (1986)
	Seed plant: *Phaseolus vulgaris*	9pcy	Red	NMR	1–99	−7	−8		P700+	Moore et al. (1991)
	Fern: *Dryopteris crassirhizoma*	1kdj	Ox	1.70	1–102	−5		cyt f[a]	in PSI (1)	Kohzuma et al. (1999)
		1kdi	Red	1.80	1–102		−6			Kohzuma et al. (1999)
	Green alga: *Ulva pertusa*	1iuz	Ox	1.60	1–100	−5	−6			Shibata et al. (1999)
	Green alga: *Chlamydomonas reinhardtii*	2plt	Ox	1.50	1–100	−5	−6			Redinbo et al. (1993)
	Green alga: *Enteromorpha prolifera*	7pcy	Ox	1.80	1–100	−5	−6			Collyer et al. (1990)
	Cyanobacteriurn: *Prochlorothrix hollandica*	1b3I	Ox	NMR	1–97	+3	+2			Babu et al. (1999)
	Cyanobacterium: *Phormidium laminosum*	1baw	Ox	2.80	1–105	−2	−3			Bond et al. (1999)
	Cyanobacterium: *Anabaena variabilis*	1nin	Ox	NMR	1–105	+2	+1			Badsberg et al. (1996)
	Cyanobacterium: *Synechocystis* sp.	1pcs	Ox	2.15	1–101	−1	−2			Romero et al. (1998)
Azurin	*Alcaligenes xylosoxidans* azurinI	1rkr	Ox	2.45	1–129	+3	+2			Li et al. (1998)
	Alcaligenes xylosoxidans azurinII	1arn	Ox	2.60	1–129	+2	+1	cyt	Nitrite	Dodd et al. (1995)
	Alcaligenes denitrificans	2aza	Ox	1.80	1–129	+1	0	c551[b]	reductase[b,c]	Baker (1998)
	Pseudomonas aeruginosa	4azu	Ox	1.90	1–128	0	−1			Nar et al. (1991)
	Pseudomonas fluorescens (Biotype A)	1joi	Ox	2.05	1–128	+1	0		Or cyt	Zhu et al. (1994)
	Pseudomonas putida	1now	Ox	1.92	1–128	+2	+1	Or AADH[b]	Oxidase[b]	Chen et al. (1998)
Pseudoazurin	*Alcaligenes faecalis*	8paz	Ox	1.60	1–123	+1		n.d.[d]	Cu-NIR	Libeu et al. (1997)
		3paz	Red	1.73	1–123		0		(green)[e]	Libeu et al. (1997)
	Achromobacter cycloclastes	1zia	Ox	1.54	1–124	+2		n.d.[d]	Cu-NIR	Inoue et al. (1993)
		1zib	Red	2.00	1–124		+1		(green)	Inoue et al. (1993)
	Paracoccus denitrificans (subsp. *Thiosphaera pantotropha*)	1adw	Ox	2.50	1–123	−3	−4	n.d.[d] MADH[e] or	cyt cd1[e]	Williams et al. (1995)
	Methylobacterium extorquens	1pmy	Ox	1.50	1–123	+3	+2	Methanol DH	c-type cyt[e]	Inoue et al. (1994)
Amicyanin	*Paracoccus denitrificans*	1aac	Ox	1.31	1–105	−1			cyt c55li	Durley et al. (1993)
		2rac	Red	1.30	1–105		−2	MADH	or c-type	Zhu et al. (1998)
	Paracoccus versutus	aminmr[f]		NMR	1–106	−2	−3		cyt	Kalverda et al. (1994)
Rusticyanin	*Thiobacillus ferrooxidans*	1rcy	Ox	1.90	4–155	+2		cyt c552	cyt oxidase	Walter et al. (1996)
		1a3z	Red	1.90	4–155		+1			Walter et al. (1996)
CBP	*Cucumis sativus*	2cbp	Ox	1.80	1–96	+8	+7	n.d.[d]	n.d.[d]	Guss et al. (1996)
Stellacyanin	*Cucumis sativus*	1jer	Ox	1.60	1–109	−2	−3	n.d.[d]	n.d.[d]	Hart et al. (1996)

[a] cyt f and P700+ are redox partners for all the plastocyanins. Plastocyanins from bacteria are also able to bind cytochrome oxidase.
[b] When cytochrome c551 is the donor, a nitrite reductase is the acceptor, while cytochrome oxidase is the acceptor when AADH is the donor.
[c] Cu-NIR (blue) is the nitrite reductase interacting with azurins in *A. xylosoxidans*, while the heme-containing cytochrome cd1 binds to all the other azurins listed.
[d] Not determined.
[e] Pseudoazurins bind to Cu- and heme-containing NIRs and probably also to deaminases and c-type cytochromes in methylotrophic bacteria.
[f] This structure was kindly provided by Dr. M. Ubbink from the Leiden Institute of Chemistry (Netherlands).

1998). First, an encounter complex is formed in which the electrostatic complementarity between the two partners is maximized; this is achieved by interaction of the plastocyanin "eastern" site with the cytochrome f heme site. Then a rearrangement of the complex takes place to optimize the conformation for electron transfer so that the plastocyanin Cu-site faces the cytochrome f heme-site and the shortest distance between the two metal ions is obtained. In light of this proposed mechanism, two regions were analyzed: the "northern" and the "eastern" sites. The results reported in Figure 2 and Kinemages 2–5 in Supplementary material in the Electronic Appendix highlight the differences in the hydrophobic and electrostatic properties of the cyanobacterial and the eukaryotic plastocyanins.

A hydrophobic patch is present at the "northern" site in both the eukaryotic and cyanobacterial plastocyanins, but it is more prominent in the latter. The overall electrostatic potentials of plant plastocyanins are much more negative than those of cyanobacterial ones, reflecting the differences in their total net charges (see Table 1). In particular, an increase in negative charge with respect to the cyanobacterial proteins is found in the eukaryotic plastocyanin "eastern" sites (see Fig. 3) due to two highly conserved negatively charged sequence segments, corresponding to residues 42–45 and 59–61 in spinach plastocyanin.

Interestingly, from sequence analysis and experimental studies, Bendall et al. (Bendall et al., 1999; Carrell et al., 1999) and Hibino et al. (1996) found that effective charges in eukaryotic and cyanobacterial plastocyanins and their corresponding redox partners tend to be reversed, although these proteins probably evolved from a common ancestor. It seems probable that plastocyanins and their partners in plants developed specific mutual binding specificity and that, on the contrary, the interaction between cyanobacterial proteins remained less specific. In any case, this supports the important role played by long range molecular recognition in the overall electron transfer processes mediated by both eukaryotic and cyanobacterial plastocyanins.

Further, our analysis shows that the electrostatic and hydrophobic features of the cyanobacterial plastocyanins are more similar to those displayed by azurins and amicyanins than to those of eukaryotic plastocyanins, and therefore it can be suggested that different binding and/or electron transfer processes characterize the two types of plastocyanins. In this respect, the fact that the "eastern" site shows the most clearly defined cluster for the eukaryotic plastocyanins (see Kinemage 5A) implies that this site is most important, perhaps only important, for the eukaryotic plastocyanin subfamily. However, its influence in vivo is unclear as electrostatic interactions will be modulated by the environment of the chloroplast and there is evidence that mutation of charged residues in the basic patch of cytochrome f has less effect on electron transfer in vivo than in vitro (Soriano et al., 1998).

Fern plastocyanin: A special case

Although from sequence analysis, the plastocyanin from the fern, *Dryopteris crassirhizoma*, is identified as a plastocyanin, it lies at the edge of the cluster of plastocyanin sequences in our pairwise comparison (Fig. 2A; Kinemage 1). The fern plastocyanin has MIFs with features peculiar to itself that are roughly intermediate between those of cyanobacterial and other eukaryotic plastocyanins (Fig. 2B,C; Kinemages 2, 3). Thus, from sequence and MIF analysis, the fern plastocyanin bears no clear close relation to the algal plastocyanins although algae are the evolutionary predecessors of ferns.

The hydrophobic MIF of fern plastocyanin is more similar to those of cyanobacterial than to those of eukaryotic plastocyanins. Moreover, although it has a total net charge of -5e and -6e in its oxidized and reduced states, respectively, the fern plastocyanin lacks the highly negative patch at the "eastern" site that is typical of eukaryotic plastocyanins. An acidic patch is, however, present in the fern plastocyanin but it is closer to the "northern" site. Kohzuma et al. (1999) suggested that the acidic site and the copper site are equally efficient for electron transfer in *D. crassirhizoma* plastocyanin. Thus, it seems that all the recognition properties identified in the previous section for cyanobacterial and eukaryotic plastocyanins are present in fern plastocyanins.

Plastocyanins from Silene pratensis and Synechococcus sp.: Test cases

Recently, the reduced and oxidized structures of the plastocyanins from the eukaryote *Silene pratensis* (Sugawara et al., 1999) and from the cyanobacterium *Synechococcus sp*. (Inoue et al., 1999) have been solved. Although these structures were not included in our analysis, they were used to check the consistency of our model. The *silene* plastocyanin has MIFs (data not shown) similar to those of the plastocyanins from plants and algae used in the analysis. The plastocyanin from *Synechococcus sp.* has MIFs (data not shown) much more similar to those of cyanobacterial plastocyanins, although it has different structural features, due to a shorter loop in the "eastern" region. The area around Tyr83 (spinach plastocyanin numbering) is, interestingly, overall neutral and, Tyr83 is involved in π-π stacking with an arginine (Inoue et al., 1999). This provides further evidence for the greater diversity of the "eastern" site in cyanobacterial than eukaryotic plastocyanins, suggesting that the "eastern" site in cyanobacterial plastocyanins is less likely to be involved in redox partner recognition and electron transfer. In summary, the results obtained for these two test cases provide support for the reliability of our analysis procedure and conclusions.

Azurin subfamily

The overall architecture of azurins resembles that of plastocyanins, with the additional presence of a "back flap" formed by two α-helices located between the fifth and sixth β-strands (Fig. 1). The presence of a disulfide bridge connecting the first four β-sheets at the opposite end of the Cu-site and of a fifth Cu-ligand (a glycine carbonyl oxygen) are common to all the known azurins and differentiate them from the other cupredoxins. Subtle structural differences between the azurins resulted in assignment of different protonation states for some of the histidine residues (see Materials and methods).

Azurins are found in bacteria. They participate in the oxidative deamination of primary amines and also in denitrification processes by shuttling electrons from aromatic amine dehydrogenase (AADH) to cytochrome oxidase and from some c-type cytochromes to nitrite reductases (NIRs) (see Table 1) (Chen et al., 1998; Dodd et al., 1998). Copper-containing and heme-containing NIRs (cytochromes cd1) are electron acceptors for different azurins (van de Kamp et al., 1990; Sykes, 1994; Chen et al., 1998).

Azurins: Importance of the "northern" site

From analysis of the electrostatic features over the complete protein surfaces (Fig. 2C), no electrostatic interaction field feature is highly conserved in the azurin subfamily. However, the picture

is different if the "northern" site is considered. This is the most interesting site for investigating the MIFs in azurins, as it has been proposed to mediate both redox partner binding and the electron transfer processes in these proteins (van de Kamp et al., 1990).

Analysis of the "northern" site reveals the presence of a large conserved hydrophobic region (Fig. 2B; Kinemage 2), that might be important for electron transfer. It also reveals some shared electrostatic features (Fig. 2D; Kinemage 4), supporting the idea that the "northern" region might also be the recognition site.

Experimental support for the involvement of the Cu-site in both recognition and electron transfer processes is found in the dimeric X-ray structure of azurin from *Pseudomonas putida*, where the Cu-site of one azurin faces the Cu-site of the second azurin (Chen et al., 1998), and in the kinetic analysis of the electron self-exchange rate in azurins from *Pseudomonas aeruginosa*, where it is demonstrated that the introduction of charges in the "northern" site adversely affects the self-exchange rate (Van Pouderoyen et al., 1994).

Azurins: Two proteins in A. xylosoxidans

Two different azurins, called azurin I and azurin II, are expressed in the bacterium *A. Xylosoxidans*. They are both thought to be electron donors for the same Cu-NIR (Dodd et al., 1995). Although the sequence identity between these two azurins is relatively high (about 67%), azurin I shares higher sequence identity with *P. aeruginosa* azurin (73%) and azurin II has 85% sequence identity with *Alcaligenes denitrificans* azurin. This suggests that these two azurins might play or have played different roles in the same organism.

The results of our analysis show that, although displaying no overall similarity (Fig. 2C; Kinemages 3A, 3B), the molecular electrostatic potentials at the "northern" sites of azurins I and II are more than 95% similar (Fig. 2D; Kinemage 4). This is consistent with experimental information (Dodd et al., 1995) and supports the hypothesis that the two azurins can bind to the same blue Cu-NIR through their reduced copper site.

On the other hand, the identity of the binding partner(s) is unclear for the azurins from the *Pseudomonas* species and from *A. denitrificans*, which cluster away from the *A. xylosoxidans* azurins when the electrostatic potential at the "northern" site is analyzed (Fig. 2D; Kinemage 4).

Pseudoazurin subfamily

The architecture of pseudoazurins consists of a "plastocyanin-like" fold with two additional α-helices in the C-terminal region (Fig. 1). These cupredoxins are involved in denitrification processes in potent denitrifying bacteria, where their expression is enhanced when the host organism is grown under denitrifying conditions (Leung et al., 1997). Pseudoazurins participate in a wide range of electron transport reactions and are able to interact with a number of structurally different proteins, including cytochrome cd1, Cu-NIR and cytochrome oxidase (Inoue et al., 1994; Williams et al., 1995; Kukimoto et al., 1996; Leung et al., 1997).

Pseudoazurins and azurins: Similarities and differences

Although the hydrophobic field at the pseudoazurin Cu-site is weaker than that displayed by azurins, a conserved hydrophobic area on the protein surface is found only at the "northern" site, suggesting that the electron transfer pathway may cross this region (Williams et al., 1995). For this cupredoxin subfamily, the region around the copper is also considered to be important for binding of both the redox partners, although most of the data relate to the binding of the known electron acceptor Cu-NIRs (Kukimoto et al., 1996).

Azurins I and II from *A. xylosoxidans* and pseudoazurins from *A. faecalis* and *A. cycloclastes* donate electrons to Cu-NIRs that are structurally similar but display different spectroscopic properties (Dodd et al., 1998). The azurins and pseudoazurins show different overall electrostatic properties (Figs. 2C, 3; Kinemage 3), but are similar at the copper site, especially in their reduced states (Kinemage 4B). There is a striking dipolar distribution of the molecular electrostatic potential of pseudoazurin, which is highly positive at the copper site and highly negative on the opposite side of the protein (Fig. 3). Azurins have a weakly positively charged region at the "northern" site.

Interestingly, the green and blue Cu-NIRs display electrostatic properties that complement those of pseudoazurins and azurins, respectively (with the green Cu-NIRs having much greater net negative charge). The charge complementarity of azurins and blue Cu-NIRs, and of pseudoazurins and green Cu-NIRs, which is reflected in the MIF analysis, provides an explanation for the different experimental binding specificities of azurins and pseudoazurins for Cu-NIRs (Dodd et al., 1998).

Amicyanin subfamily

The overall fold of amicyanin is very similar to that of plastocyanin. The main difference is a large extension in the N-terminus of amicyanin (Fig. 1). Amicyanins shuttle electrons from MADH to a c-type cytochrome in the methylamine-oxidizing chain of methylotropic bacteria.

In addition to the amicyanin structures used and reported in Table 1, the crystal structure of the complex of amicyanin from *P. denitrificans* and its partners is known (Chen et al., 1994). The "northern," the "eastern," and the "ami/cytc551i" sites are all involved in formation of the amicyanin ternary complex. Our analysis, however, suggests different relative importances for these sites in the interaction of amicyanins and their redox partners.

Amicyanins: Similarity to pseudoazurins via the "northern" site

Both the amicyanin structures have a highly hydrophobic region on the "northern" site, which is involved in MADH binding in the ternary complex and which is probably important for both recognition and electron transfer processes.

Although amicyanins are classified together with the plastocyanins in the structure-sequence analysis (see Fig. 2A; Kinemage 1), their electrostatic potential distributions are highly dipolar and similar to those of the pseudoazurins (Fig. 3). As a consequence, amicyanins and pseudoazurins generally belong to the same cluster in the distributions obtained from the electrostatic potential analyses on the complete skin (Fig. 2C; Kinemage 3) and at the Cu-site (Fig. 2D; Kinemage 4) of the proteins.

Interestingly, there is experimental evidence (Inoue et al., 1994) that a pseudoazurin is expressed instead of amicyanin in *Methylobacterium extorquens*, when this organism is grown in the presence of methylamine and large amounts of copper. Since the bacterium is able to survive, even though the protein primarily involved in methylamine metabolism is absent, it has been suggested that the pseudoazurin substitutes for the amicyanin in the oxidative process. It is also worth noting that both an amicyanin

and a pseudoazurin are expressed in the *P. denitrificans* subspecies (see Table 1) (Moir et al., 1993), whose electrostatic potential distributions have similarity index values of 0.75 for the whole skin and 0.94 similar for the Cu-site region.

Thus, the results of our analysis, highlighting the similarities in the electrostatic potential distributions of amicyanins and pseudoazurins, are consistent with the available experimental data and support the hypothesis that these two proteins can act as isofunctional proteins under particular environmental conditions.

Amicyanins: Outliers at the "eastern" site

At the "eastern" site, His91 of the amicyanin from *P. denitrificans* is close to Tyr83 of spinach plastocyanin in the structural superposition (Fig. 1) and is at the MADH/amicyanin interface in the crystal structure of the complex. Position 91 is occupied by a Tyr in amicyanin from *Paracoccus versutus*. It is possible that the "eastern" site residue 91 is the entry or exit point for electrons in amicyanins (Chen et al., 1994). In Kinemage 5A, though, the amicyanins are outliers: if the "eastern" site is important for the recognition of MADH, then the amicyanins are probably the only partners, among the cupredoxins, for this protein.

Amicyanins: No common pattern at the "ami/cyt c551i" site

At the "ami/cyt c551i" site (Kinemage 5B), no clear trend is seen. The two amicyanins do not have very similar features in this region. Thus, a common role for the "ami/cyt c551i" site in all the amicyanins is not found. This is consistent with the available experimental information. Formation of the complex between amicyanin and MADH from *P. denitrificans* has been reported to precede the binding of the electron acceptor cytochrome *c* (Chen et al., 1994; Zhu et al., 1998). It has been suggested that the oxidized amicyanin is the only active form and that the reduced protein can bind cytochrome *c* only if complexed with MADH, due to the flipping of a histidine Cu-ligand (Zhu et al., 1998). A different hypothesis has been advanced about the interaction between the amicyanin from *P. versutus* and its redox partners, suggesting that no ternary complex is formed in vivo and that this amicyanin acts as a shuttle between MADH and a c-type cytochrome (Ubbink et al., 1994).

In conclusion, it appears that from the data available at present, the "ami/cyt c551i" is not an important binding region for most of the blue copper proteins, including the amicyanins.

Rusticyanin and phytocyanin subfamilies

To date, each of the rusticyanin, CBP, and stellacyanin subfamilies have only one solved protein structure. Probably for this reason, they are often classified as outliers in our analyses.

Rusticyanin: Similarities to azurins, pseudoazurins, and plastocyanins

The rusticyanin structure is the largest of all the known blue copper proteins and has a very low sequence identity with all the other proteins considered in this study (Fig. 2A; Kinemage 1). In the literature, rusticyanin is described as being homologous to the cupredoxins at its C-terminus (Fig. 1) and sharing some structural similarities with the type-I copper domain in Cu-NIRs (Harvey et al., 1998). Because of its unusual structure, rusticyanin has an uncommonly high redox potential (the highest among the cupredoxins) and is stable under extreme acidic conditions (Harvey et al., 1998). Its electron donor is likely to be a c-type heme cytochrome, probably cytochrome c552, and its electron acceptor is an a-type heme-containing cytochrome, probably cytochrome oxidase (Yamanaka & Fukumori, 1995).

Interpreting the results of our analysis for rusticyanin is difficult due to both its unusual structure and the small amount of experimental data available. Hydrophobic areas are present over the complete surface of the protein, differentiating rusticyanin from all the other cupredoxins (Fig. 2B; Kinemage 2) and suggesting that a different electron transfer mechanism might characterize this protein. In contrast, the electrostatic properties of rusticyanin are similar to those of cyanobacterial plastocyanins and azurins (Fig. 2C; Kinemages 3A, 3B), consistent with the fact that all these proteins can bind to cytochrome oxidase (see Table 1). Further support for this is found in the analysis of the "eastern" site (Kinemage 5A), where rusticyanin and the cyanobacterial plastocyanins again show similar behavior. This implies that, for rusticyanin, the "eastern" site might be important for the binding of cytochrome oxidase.

On the other hand, the electrostatic features of the "northern" site of rusticyanin are similar to those of the pseudoazurins and the azurins from *A. xylosoxidans* (Fig. 2D; Kinemages 4A, 4B). This result is consistent with the fact that rusticyanin and the azurins can accept electrons from a c-type heme cytochrome.

Phytocyanins: Unusual properties

CBP and stellacyanin are plant specific proteins belonging to the phytocyanin subgroup. They have 33% sequence identity and share the same fold, the "phytocyanin-like" fold (Hart et al., 1996), which is a variant of the "plastocyanin-like" fold with different packing of the β-strands and a disulfide bridge that plays a structural role at the "northern" site (Fig. 1). The main structural differences between these two proteins are in the Cu-site, since in stellacyanin, the methionine Cu-ligand is substituted by a glutamine. Furthermore, it is known that while CBP is a single domain protein, stellacyanin has a chimeric structure, consisting of a "phytocyanin-like" domain and a glycosylated domain that is probably important for binding to the cell wall (Nersissian et al., 1998).

Knowledge about CBP and stellacyanin is very limited. CBP is an extremely basic, nonglycosylated single domain protein, probably located in the endoplasmic reticulum. Recently, evidence has been provided supporting an unusual role for stellacyanin, namely, that it is involved in primary plant defence processes by catalyzing redox reactions with small compounds or lignin formation, rather than mediating electron transfer processes (Nersissian et al., 1998).

CBP: Electron shuttle protein with peculiar electrostatic properties

The hydrophobic properties of CBP are similar to those of azurins and amicyanins (Fig. 2B; Kinemage 2), supporting a similar electron transfer mechanism. In contrast, its overall electrostatic properties are very different from those of all the other proteins (Fig. 2C; Kinemage 3) and such a diversity cannot be explained simply by its being distantly related in sequence to the other proteins (Fig. 2A; Kinemage 1). Furthermore, the recognition properties of CBP are also different from those of stellacyanin, even though these two protein structures are from the same organism and share the same fold. All the results are consistent with the highly positive electrostatic potential characterizing the CBP, which is also reflected in the value of the total charge (+8e and +7e for the oxidized and the reduced states, respectively, see Table 1).

Stellacyanin: An outlier

Although it has a hydrophobic patch at its Cu-site, stellacyanin behaves as an outlier in the analysis of the hydrophobic properties (Fig. 2B; Kinemage 2). On the other hand, its behavior in the electrostatic field analysis is difficult to rationalize. The molecular electrostatic potential of stellacyanin is, overall and at the "eastern" site (Fig. 2C; Kinemages 3, 5A), similar to that of eukaryotic plastocyanins, especially of fern plastocyanin, while at the "northern" site (Fig. 2D; Kinemages 4) it is somewhat similar to that of the other cupredoxins.

A negatively charged region is present, as for eukaryotic plastocyanins, at the "eastern" site. His49 is positioned in the middle of this region, close to Tyr83 in spinach plastocyanin in the structural superposition. Based on the results from experiments on electron transfer in the stellacyanin from *Rhus vernicifera*, it has been advanced that this histidine is the entry and exit point for electrons (Hart et al., 1996).

At the copper site, the potential is weakly positive due to the exceptionally high degree of solvent exposure of the two histidines that bind to the copper. A second important difference compared to the other blue copper proteins is that the fourth ligand to the copper is a glutamine instead of a methionine. These structural peculiarities might be the reason for the low redox potential of stellacyanins (which is the lowest amongst the cupredoxins) and support the hypothesis that these proteins are redox active proteins involved in the metabolism of small molecules, rather than electron shuttle proteins (Nersissian et al., 1998). However, experimental information about the chimeric structure of stellacyanin should also be taken into account. The glycoprotein-like domain probably anchors the protein to the cell wall so that the C-terminal region of the "phytocyanin-like" domain faces the membrane (Nersissian et al., 1998). Clearly, the MIFs of stellacyanin, in its integral form, would be different from those computed considering the protein as a single-domain soluble protein. This hinders the possibility of making a hypothesis about the nature of the redox partners of stellacyanin by comparison with the other blue copper proteins.

Concluding remarks

Comparative analysis of the 3D molecular interaction fields of a family of proteins by similarity indices is a useful tool to gain insights into the recognition features of the proteins, and how these have changed with evolution. This method is particularly suited for large-scale analyses, which will become increasingly important in structural and functional genomics projects. For these, rapid automated and reliable techniques are required to perform comparisons of large numbers of experimentally-determined and modeled protein structures. The usefulness of the approach for analyzing modeled protein structures was recently demonstrated by Blomberg et al. (1999) in their study of PH domains.

The focus of this paper is the inspection and comparison of the molecular hydrophobic and electrostatic potentials of the structurally characterized members of the blue copper protein family. For these proteins, the analysis of the electrostatic potential proved to be more revealing than that of the hydrophobic potential, although the latter clearly showed the presence of a hydrophobic patch in the region around the copper that is common to all the blue copper proteins. Moreover, from our analysis, it is evident that the similarity in the hydrophobic properties can be approximately deduced from the protein sequence, since similar hydrophobic properties are correlated with similar sequences. In contrast, the analysis of the electrostatic properties provided information which is complementary to that from analysis of sequences and structures.

The electrostatic potential analysis highlighted the low specificity of binding displayed by many of the blue copper proteins. Evidence is found that some proteins belonging to different subfamilies show similar electrostatic features. In particular, the pseudoazurins and the amicyanins expressed from the same bacterial species grown under different conditions seem to behave as isofunctional proteins. Likewise, the *A. xylosoxidans* azurins and the pseudoazurins expressed in the *Alcaligenes* and *Achromobacter* species can bind to similar electron acceptor proteins via the "northern" site, although they have different binding specificity for their particular redox partners. On the other hand, the analysis highlighted differences in the molecular recognition properties of the cyanobacterial and the eukaryotic plastocyanins, and the peculiar character of the fern plastocyanin.

In conclusion, the method presented provides semiquantitative measures, and thus classifications, of the recognition properties of blue copper proteins. The results suggest experiments to obtain further insights into the physiological functions of the proteins. In further studies, this will be applied to assess the results from mutagenesis experiments and to explain data connected with the electron transfer self-exchange processes taking place in biological redox systems.

Materials and methods

Materials

X-ray and NMR structures of selected blue copper proteins were taken from the Brookhaven Protein Data Bank (PDB) (see Table 1). A representative structure from a set of 14 NMR structures of amicyanin from *P. versutus* (formerly, *Thiobacillus versutus*) (Kalverda et al., 1994) was kindly provided by Dr. M. Ubbink and is referred to as "aminmr" in Table 1. The structures of the two known complexes of blue copper proteins with their redox partners were taken from the Protein Data Bank (PDB codes: 2mta for amicyanin and 2pcf for plastocyanin).

Methods

Sequence analysis

Structure-based pairwise sequence alignments were calculated using MODELLER version 4 (Sali & Blundell, 1993). From these alignments, the percentage sequence identity was computed using MODELLER as

$$id(a,b) = 100 \times N/n$$

where N is the number of identical residues in the aligned sequences of protein a and b, and n is the number of residues in the shortest sequence. While the structure-based sequence alignments contain gaps and were constructed using gap penalties, these do not contribute to the computed values of $id(a,b)$.

A distance matrix was computed based on the pairwise $id(a,b)$ values to compare each protein with all the others:

$$D(a,b) = \sqrt{(1 - id(a,b)/100)}$$

where $D(a,b)$ is the distance between the proteins a and b. The matrix, thus obtained, allows a projection of the molecules in 3D space according to their sequence identities. Each point in the 3D space represents a single protein. This 3D projection is obtained by choosing the first two points corresponding to those proteins (1 and 2) for which the distance $D(1,2)$ is the greatest. $D(1,2)$ is then used for normalization of all other distances. Point 3, corresponding to protein 3, is chosen so that the area of the triangle formed by points 1, 2, and 3 is the maximum possible and point 4, representing protein 4, is chosen so that the volume of the tetrahedron formed by points 1, 2, 3, and 4 is the maximum possible. Thus, 4 points are chosen having coordinates (0,0,0), (1,0,0), (x1,x2,0), (x3,x4,x5), where x1-x5 are calculated from the six pairwise distances $D(1,2)$, $D(3,1)$, $D(3,2)$, $D(4,1)$, $D(4,2)$, $D(4,3)$. The other proteins are then projected onto this defined 3D space with coordinates determined from their $D(a,b)$ values. The 3D projection can be visualized with the MAGE program (Richardson & Richardson, 1992) (at http://kinemage.biochem.duke.edu) as described by Tomic et al. (Tomic et al., 1998a, 1998b).

Structure preparation and superposition

When more than one crystal structure was known for the same protein in the same organism, only one was selected for analysis. The criteria for structure selection were (1) highest resolution; (2) most recently solved; and (3) smallest number of differences in sequence from the wild-type protein.

For the proteins solved by NMR, the average structure was used when this was deposited in the Protein Data Bank. Otherwise, the structure used was a representative structure from the most populated cluster selected by the automated procedure implemented in the program NMRCLUST (Kelley et al., 1996).

When two different structures of a given protein were known for its reduced and oxidized states, then both of them were included in the analysis (see Table 1). On the other hand, when only one form of the protein was known, then the same structure was used for the analysis of both the reduced and the oxidized states, on the assumption that the structural differences between these two states are minimal (see Table 1). This assumption is reasonable, as the root-mean-square deviations between the experimentally determined structures of oxidized and reduced forms of blue copper proteins are in the range of 0.16–0.32 Å. Nevertheless, the method used to compare the protein interaction fields was tested to check its sensitivity to the choice of the protein structures (see Results).

All the proteins analysed had wild-type sequences. If, for a given protein, only a structure of a mutant was available, it was mutated with the InsightII software package (MSI, San Diego, California) to the wild-type sequence (as given in the SWISSPROT database).

In both the oxidized and reduced crystal structures of rusticyanin (PDB entries: 1rcy and 1a3z), the initial five residues (GTLDS) are lacking. The presence of the acidic residue (Asp) at position 4 could significantly influence the local distribution of the electrostatic potential. Thus, Asp4 and Ser5 were added with the Quanta software package (MSI). The two added residues and the adjacent residues that have very high *B*-factors (Thr6 in 1rcy and Thr6–Trp7–Lys8 in 1a3z) were energy minimized (500 steps of steepest descent followed by 1,000 steps of conjugate gradient) with the CHARMm program implemented in Quanta.

When side chains were disordered in the coordinate files, the conformation with the highest occupancy was selected. Water molecules and any ions in the crystal structures were removed.

The WHATIF program (v. 19990307-1124) (Vriend, 1990) was used to add polar hydrogens to the structures.

The structures were superimposed with the Quanta program (MSI) using a standard least-squares fitting algorithm. The fit was optimized on all atoms of the copper site and on Cα atoms of the β-sheet secondary structure that is conserved in all the blue copper protein subfamilies. Figure 1 shows the structure-based sequence alignment of eight blue copper proteins representative of the seven different subfamilies considered in this study.

Molecular hydrophobic potential calculation

The GRID program, version 17 (Molecular Discovery Ltd., Oxford, UK) was used to compute the hydrophobic fields of the blue copper proteins. The "DRY" hydrophobic probe was employed. A grid of $110 \times 110 \times 110$ Å^3 with a 1.0 Å spacing centred on the center of mass of the superimposed protein structures was used.

Molecular electrostatic potential calculations

The University of Houston Brownian Dynamics (UHBD) program, version 6.1 (Madura et al., 1995), was used to compute the molecular electrostatic potentials of the cupredoxins.

The N- and C-terminal residues were treated as charged. The ionizable residues were considered in their usual protonation states at pH 7. The histidine residues were assigned, using the WHATIF program, to be either in their neutral or doubly protonated forms depending on their hydrogen-bonding environment. The majority of the protein structures were assigned only neutral forms of histidine. The exceptions are stellacyanin (His85 in PDB entry 1jer), amicyanin from *P. denitrificans* (His36 in both PDB entries 1aac and 2rac) and all the azurins (His32 in 1arn and 2aza, His35 in 1joi, 1nwo, 1rkr and 4azu).

The OPLS (Jorgensen & Tirado-Rives, 1988) nonbonded parameter sets for atomic charges and radii were assigned to the protein residues. The copper radius was set to 1.2 Å, as in the Amber (v. 4.1) parameter set. Different partial atomic charge sets suggested in the literature (Ullmann, 1998; De Kerpel & Ryde, 1999) were tested for the parameterization of the Cu-site, but varying the distribution of charges proved not to affect the results of the analysis significantly. The charge parameters were thus assigned to the copper site (Cu and its ligands) using a simple distribution algorithm, developed on the basis of that proposed by Libeu et al. (1997). The formal charge $+1/+2$e for the Cu+1/Cu+2 states was partially redistributed over the copper ligands, so that charges of $+0.5$e and $+1.5$e were assigned to the copper in its reduced and oxidized states, respectively, and the remaining charge of $+0.5$e was evenly distributed among the Cu ligands. Thus, in the plastocyanin, pseudoazurin, amicyanin, rusticyanin, and CBP structures, a charge of $+0.125$e was added to the OPLS default values for each of the two ND1(His) Cu-ligands and for the SD(Met) and the SG(Cys) Cu-ligands. In stellacyanin, the Cu-ligand methionine is substituted by a glutamine, thus a charge of $+0.125$e was assigned to the OE1(Gln) atom. Azurins are characterized by the presence of a fifth Cu-ligand, which is the backbone carbonyl oxygen of a glycine. In this case, a charge value of $+0.1$e was assigned to each of the five Cu-ligands.

A grid dimension of $110 \times 110 \times 110$ Å^3 was assigned together with a 1.0 Å grid spacing for computing the electrostatic potential by finite difference solution of the linearized Poisson–Boltzmann equation. The grid was centered on the global center of mass of the superimposed structures.

The dielectric constants of the solvent and the protein were set to 78 and 2, respectively. The dielectric boundary was determined from the van der Waals surface of the protein and dielectric boundary smoothing (Davis & McCammon, 1991) was implemented.

The molecular electrostatic potential grids were computed at two different values of the ionic strength, 0 and 150 mM at a temperature of 300 K.

PIPSA—protein interaction properties similarity analysis

For each pair of proteins a and b, the molecular potentials, $\phi_a(i,j,k)$ and $\phi_b(i,j,k)$, computed on a 3D grid, were compared by calculating the Hodgkin similarity index. This index provides a measure of the similarity between the magnitudes and distributions of the molecular potentials of the two proteins compared.

$$SI_{\mathrm{HODGKIN}}(a,b) = 2(M_a, M_b)/(M_{a^2} + M_{b^2}).$$

The scalar products (M_a, M_b), M_{a^2}, M_{b^2} represent the sum of products of values calculated for a given molecular potential M (molecular electrostatic or hydrophobic potential) on grid points (i,j,k):

$$(M_a, M_b) = \sum_{i,j,k} \phi_a(i,j,k)\,\phi_b(i,j,k)$$

where the summation is over the grid points within a defined region of interest. This region, called the "skin," is chosen to be at a distance σ from the van der Waals surface of each protein and to have a thickness δ. Thus, the SIs for comparison of two proteins are calculated for grid points within the intersection of their skins. The parameters σ and δ were chosen so that the region where the potentials are compared is not so close to the protein surfaces as to be highly sensitive to small changes in protein structure and not so far that only the major components of the potentials (e.g., electrostatic monopoles) can be detected. In the present study, values of $\sigma = 3$ Å and $\delta = 4$ Å were used to define the skins for the electrostatic potential analysis. For the hydrophobic potential analysis, a distance $\sigma = 2$ Å (with $\delta = 4$ Å) was chosen because hydrophobic interactions are effective at a shorter range than electrostatic interactions. The SI values lie in the range -1 to 1, with values near to 1 implying that the proteins have highly similar potentials on the overlapping skins and values near to -1 implying that the potentials have inverted distributions. The details of the method have been described by Blomberg et al. (1999).

The analysis of the molecular potential similarity was performed for different regions: (1) the potentials were compared in the intersecting regions of the complete skins of the proteins and (2) the analysis was restricted to particular chosen regions of the skins. For the latter, a vector was chosen having its origin at the centre of mass of the superimposed structures and pointing toward the region to be studied. Only the intersection of those parts of the skins inside a conical region centered on the vector and with a 30° angular extent was considered.

The following three regions, chosen because of their possible importance either for binding or for electron transfer processes, were defined for the analysis of the molecular potentials:

1. the copper or "northern" site;
2. the so-called "eastern" site around Tyr83 in plastocyanin from spinach;
3. the "ami/cyt c551i" site around Thr32 in amicyanin from *P. denitrificans*.

The comparison of the molecular potential SIs was carried out by computing a distance matrix consisting of $D(a,b)$ values for all protein pairs. $D(a,b)$ is the distance between proteins a and b defined as

$$D(a,b) = \sqrt{1 - SI(a,b)}$$

where $SI(a,b)$ is the Hodgkin SI calculated on the intersection of the skins of proteins a and b. This distance matrix was used to automatically cluster the proteins using the NMRCLUST program (Kelley et al., 1996). The distribution of the proteins according to the distance matrix was projected into 3D space and visualised with the MAGE program (as described in "Sequence analysis" in Materials and methods). The extent to which the information in the full distance matrix is captured in the 3D projection can be quantified by computing a Hodgkin similarity index between the full distance matrix and the 3D distance matrix. For the properties analyzed in this work, this similarity index takes values between 0.75 (for the hydrophobic fields around the copper site) and 0.94 (for the electrostatic fields over the whole skin of the oxidized proteins at 150 mM ionic strength). For the electrostatic fields of the oxidized proteins at 0 mM ionic strength, this similarity index takes values of 0.85 (whole skin) and 0.78–0.80 (three selected regions). This shows that the 3D projections capture most of the information stored in the full distance matrices and thus visual inspection of the 3D projections can be a useful aid for analysis. The lower value of this similarity measure for the 3D projection for the hydrophobic fields likely stems from the fact that their similarity indices only take positive values and high values are less common, making relationships between the proteins' hydrophobic fields more complicated than for electrostatic fields.

Supplementary material in the Electronic Appendix

This consists of:

1. 8 pairwise similarity matrices (27 × 27): 1.mat, 2.mat, 3a.mat, 3b.mat, 4a.mat, 4b.mat, 5a.mat, and 5b.mat.
2. 8 Kinemages: 1.kin (corresponding to Fig. 2A), 2.kin (corresponding to Fig. 2B), 3a.kin (corresponding to Fig. 2C), 3b.kin, 4a.kin (corresponding to Fig. 2D), 4b.kin, 5a.kin and 5b.kin, corresponding to pairwise similarity matrices 1.mat, 2.mat, 3a.mat, 3b.mat, 4a.mat, 4b.mat, 5a.mat, and 5b.mat, respectively.

Pairwise similarity matrices

1.mat: Pairwise sequence identity percentages.

2.mat: Hydrophobic potential pairwise similarity indices calculated at the Cu-site.

3a.mat and 3b.mat: Electrostatic potential pairwise similarity indices obtained from the analysis of the oxidized proteins at (a) 0 mM and (b) 150 mM ionic strength.

4a.mat and 4b.mat: Electrostatic potential pairwise similarity indices obtained from the analysis at the Cu-site at 0 mM ionic strength of (a) the oxidized and (b) the reduced proteins.

5a.mat and 5b.mat: Electrostatic potential pairwise similarity indices obtained from the analysis of the oxidized proteins at 0 mM and ionic strength at (a) the "eastern" site and (b) the "ami/cytc551i" site.

Kinemages

1.kin: 3D distribution of pairwise sequence identity. Key: light green, cyanobacterial plastocyanins; dark green, eukaryotic plastocyanins; cyan, azurins; violet, pseudoazurins; orange, amicyanins; magenta, rusticyanin; white, CBP; brown, stellacyanin.

2.kin: 3D distribution of hydrophobic potential similarity indices, obtained from the analysis at the Cu site. Color code as for 1.kin.

3a.kin and 3b.kin: 3D distribution of molecular electrostatic potential similarity indices, calculated for the oxidized proteins at (**a**) 0 mM and (**b**) 150 mM ionic strength. Color code as for 1.kin.

4a.kin and 4b.kin: 3D distribution of electrostatic potential similarity indices, obtained from analysis at the Cu-site and at an ionic strength of 0 mM of (**a**) the oxidized and (**b**) the reduced proteins. Color code as for 1.kin.

5a.kin and 5b.kin: 3D distribution of electrostatic potential similarity indices, obtained from the analysis of the oxidized proteins at an ionic strength of 0 mM at (**a**) the "eastern" site and (**b**) the "ami/cyt c551i" site. Color code as in 1.kin.

Acknowledgments

We are grateful to Dr. G.W. Canters, Dr. M. Ubbink, Dr. A. Kalverda, and Dr. A. Messerschmidt for supplying NMR and X-ray structures of amicyanins from *P. versutus* and Dr. T. Inoue for the X-ray structures of plastocyanin from *S. pratensis*. We thank Dr. D.S. Bendall for providing us with supplementary material. We thank Dr. S. Tomic and Dr. W.C. Lathe III for critical reading of the manuscript. F.D.R. is the recipient of a predoctoral grant from the University of Modena and Reggio Emilia.

References

Adman ET. 1991. Copper protein structures. *Adv Prot Chem 42*:145–197.

Babu CR, Volkman BF, Bullerjahn GS. 1999. NMR solution structure of plastocyanin from the photosynthetic prokaryote, Prochlorothrix hollandica. *Biochemistry 38*:4988–4995.

Badsberg U, Jorgensen AM, Gesmar H, Led JJ, Hammerstad JM, Jespersen LL, Ulstrup J. 1996. Solution structure of reduces plastocyanin from the blue-green alga *Anabaena variabilis*. *Biochemistry 35*:7021–7031.

Bagby S, Driscoll PC, Harvey TS, Hill HAO. 1994. High-resolution structure of reduced parsley plastocyanin. *Biochemistry 33*:6611–6622.

Baker EN. 1988. Structure of azurin from *Alcaligenes denitrificans*. Refinement at 1.8 Angstrom resolution and comparison of the two crystallographic independent molecules. *J Mol Biol 203*:1071–1095.

Baker EN. 1994. Copper proteins with type 1 sites. In: King RB, ed. *Encyclopedia of inorganic chemistry*. Chichester, UK: Wiley Interscience. pp 883–923.

Bendall DS, Wagner MJ, Schlarb BG, Soellick TR, Ubbink M, Howe CJ. 1999. Electron transfer between cytochrome f and plastocyanins in *Phormidium laminosum*. In: Peschek GA, ed. *The phototropic prokaryotes*. New York: Kluwer Academic/Plenum. pp. 315–328.

Blomberg N, Gabdoulline RR, Nilges M, Wade RC. 1999. Classification of protein sequences by homology modeling and quantitative analysis of electrostatic similarity. *Proteins 37*:379–387.

Bond CS, Wilce MCJ, Guss JM, Freeman HA, Wagner MJ, Howe CJ, Bendall DS. 1999. The structure of plastocyanin from the cyanobacterium phormidium laminosum. *Acta Crystallogr D 55*:414–421.

Carrell CJ, Schlarb BG, Bendall DS, Howe CJ, Cramer WA, Smith JL. 1999. Structure of the soluble domain of cytochrome f from the cyanobacterium *Phormidium laminosum*. *Biochemistry 38*:9590–9595.

Chen L, Durley RCE, Mathews FS, Davidson VL. 1994. Structure of an electron transfer complex: Methylamine dehydrogenase, amicyanin and cytochrome c551i. *Science 264*:86–90.

Chen Z-W, Barber MJ, McIntire WS, Mathews FS. 1998. Crystallographic study of azurin from *Pseudomonas putida*. *Acta Crystallogr D54*:253–268.

Collyer CA, Guss JM, Sugimura Y, Yoshizaki F, Freeman HC. 1990. The crystal structure of plastocyanin from a green alga, *Enteromorpha prolifera*. *J Mol Biol 211*:617–632.

Davis ME, McCammon JA. 1991. Dielectric boundary smoothing in finite difference solutions of the poisson equation: An approach to improve accuracy and convergence. *J Comp Chem 12*:909–912.

De Kerpel JOA, Ryde U. 1999. Protein strain in blue copper proteins studied by free energy perturbations. *Proteins 36*:157–174.

Demchuk E, Mueller T, Oschkinat H, Sebald W, Wade RC. 1994. Receptor binding properties of four-helix-bundle growth factors deduced from electrostatic analysis. *Protein Sci 3*:920–935.

Dodd FE, Hasnain SS, Hunter WN, Abraham ZHL, Debenham M, Kanzler H, Eldridge M, Eady RR, Ambler RP, Smith BE. 1995. Evidence for two distinct azurins in *Alcaligenes xylosoxidans* (NCIMB 11015): Potential electron donors to nitrite reductase. *Biochemistry 34*:10180–10186.

Dodd FE, Van Beeumen J, Eady RR, Hasnain SS. 1998. X-ray structure of a blue-copper nitrite reductase in two crystal forms. The nature of the copper sites, mode of substrate binding and recognition by redox partner. *J Mol Biol 282*:369–382.

Durell SR, Labanowski JK, Gross EL. 1990. Modeling of the electrostatic potential field of plastocyanin. *Arch Biochem Biophys 277*:241–254.

Durley R, Chen L, Lim LW, Mathews FS, Davidson VL. 1993. Crystal structure analysis of amicyanin and apoamicyanin from *Paracoccus denitrificans* at 2.0 Angstrom and at 1.8 Angstrom resolution. *Protein Sci 2*:739–752.

Gross EL, Curtiss A, Durell SR, White D. 1990. Chemical modification of spinach plastocyanin using 4-chloro-3,5-dinitrobenzoic acid: characterization of four singly-modified forms. *Biochim Biophys Acta 1016*:107–114.

Guss JM, Bartunik HD, Freeman HC. 1992. Accuracy and precision in protein structure analysis: Restrained least-squares refinement of the structure of poplar plastocyanin at 1.33 angstroms resolution. *Acta Crystallogr B 48*:790–811.

Guss JM, Harrowell PR, Murata M, Norris VA, Freeman HC. 1986. Crystal structure analyses of reduced (CuI) poplar plastocyanin at six pH values. *J Mol Biol 191*:361–387.

Guss JM, Merritt EA, Phizackerley RP, Freeman HC. 1996. The structure of a phytocyanin, the basic blue protein from cucumber, refined at 1.8 A resolution. *J Mol Biol 262*:686–705.

Hart PJ, Nersissian AM, Herrmann RG, Nalbandyan RM, Valentine JS, Eisenberg D. 1996. A missing link in cupredoxins: Crystal structure of cucumber stellacyanin at 1.6 A resolution. *Protein Sci 5*:2175–2183.

Harvey I, Hao Q, Duke EMH, Ingledew WJ, Hasnain SS. 1998. Structure determination of a 16.8 kDa copper protein at 2.1 A resolution using anomalous scattering data with direct methods. *Acta Crystallogr D54*:629–635.

Hibino T, Lee BH, Yajima T, Odani A, Yamauchi O, Takabe T. 1996. Kinetic and cross-linking studies on the interactions of negative patch mutant plastocyanin from *Silene pratensis* with photosystem I complexes from cyanobacteria, green algae, and plants. *J Biochem 120*:556–563.

Inoue T, Kai Y, Harada S, Kasai N, Ohshiro Y. 1994. Refined crystal structure of pseudoazurin from *Methylobacterium extorquens* AM1 at 1.5 A resolution. *Acta Crystallogr D50*:317–328.

Inoue T, Nishio N, Kai Y, Harada S, Ohshiro Y, Suzuki S, Kohzuma T, Shidara S, Iwasaki H. 1993. Crystallization and preliminary X-ray studies on pseudoazurin from *Achromobacter cycloclastes* IAM1013. *J Biochem 114*:761–762.

Inoue T, Sugawara H, Hamanaka S, Tsukui H, Suzuki E, Kohzuma T, Kai Y. 1999. Crystal structure determinations of oxidized and reduced plastocyanin from the cyanobacterium *Synechococcus* sp. PCC 7942. *Biochemistry 38*:6063–6069.

Jorgensen WL, Tirado-Rives J. 1988. The OPLS potential function for proteins. Energy minimization for crystals of cyclic peptides and crambin. *J Am Chem Soc 110*:1657–1666.

Kalverda AP, Wymenga SS, Lommen A, van de Ven FJM, Hilbers CW, Canters GW. 1994. Solution structure of the type 1 blue copper protein amicyanin from *Thiobacillus versutus*. *J Mol Biol 240*:358–371.

Kelley LA, Gardner SP, Sutcliffe MJ. 1996. An automated approach for clustering an ensamble of NMR-derived protein structures into conformationally-related subfamilies. *Protein Eng 9*:1063–1065.

Kohzuma T, Inoue T, Yoshizaki F, Sasakawa Y, Onodera K, Nagatomo S, Kitagawa T, Uzawa S, Isobe Y, Sugimura Y, et al. 1999. The structure and

unusual pH dependence of plastocyanin from the fern *Dryopteris crassirhizoma*. *J Biol Chem 274*:11817–11823.
Kukimoto M, Nishiyama M, Ohnuki T, Turicy S, Adman ET, Horinouchi S, Beppu T. 1995. Identification of interaction site of pseudoazurin with its redox partner, copper-containing nitrite reductase from *Alcaligenes faecalis* S-6. *Protein Eng 8*:153–158.
Kukimoto M, Nishiyama M, Tanokura M, Adman ET, Horinouchi S. 1996. Studies on protein-protein interaction between copper-containing nitrite reductase and pseudoazurin from *Alcaligenes faecalis* S6. *J Biol Chem 271*:13680–13683.
Lee BH, Hibino T, Takabe T, Weisbeek PJ, Takabe T. 1995. Site-directed mutagenetic study on the role of negative patches on *silene* plastocyanin in the interactions with cytochrome f and photosystem I. *J Biochem 117*:1209–1217.
Leung Y-C, Chan C, Reader JS, Willis AC, van Spanning RJM, Ferguson SJ, Radford SE. 1997. The pseudoazurin gene from *Thiosphaera pantotropha*: Analysis upstream putative regulatory sequences and overexpression in *Escherichia coli*. *Biochem J 321*:699–705.
Li C, Inoue T, Gotowda M, Suzuki S, Yamaguchi K, Kataoka K, Kai Y. 1998. Structure of azurin-I from denitrifying bacterium alcaligenes xylosoxydans NCIMB 11015 at 2.45 A resolution. *Acta Crystallogr D 54*:347–354.
Libeu CAP, Kukimoto M, Nishiyama M, Horinouchi S, Adman ET. 1997. Site-directed mutants of pseudoazurin: Explanation of increased redox potentials from X-ray structures and from calculation of redox potential differences. *Biochemistry 36*:13160–13179.
Madura JD, Briggs JM, Wade RC, Davis R, Luty BA, Ilin A, Antonsiewicz J, Bagheri MK, Scott B, McCammon JA. 1995. Electrostatic and diffusion of molecules in solution: Simulation with the University of Huston Brownian Dynamics program. *Comp Phys Comm 91*:57–95.
Manna P, Vermaas W. 1997. Lumenal proteins involved in respiratory electron transport in the cyanobacterium *Synechocystis* sp. PCC6803. *Plant Mol Biol 35*:407–416.
Moir JWB, Baratta D, Richardson DJ, Ferguson SJ. 1993. The purification of a cd1-type nitrite reductase from, and the absence of a copper-type nitrite reductase from, the aerobic denitrifier *Thiosphaera Pantotropha*; the role of pseudoazurin as an electron donor. *Eur J Biochem 212*:377–385.
Moore JM, Lepre CA, Gippert GP, Chazin WJ, Case DA, Wright PE. 1991. High-resolution solution structure of reduced french bean plastocyanin and comparison with the crystal structure of poplar plastocyanin. *J Mol Biol 221*:533–555.
Nar H, Messerschmidt A, Huber R, Van de Kamp M, Canters GW. 1991. Crystal structure analysis of oxidized Pseudomonas aeruguinosa azurin at pH 5.5 and pH 9.0. A pH-induced conformational transition involves a peptide bond flip. *J Mol Biol 221*:765–772.
Nersissian AM, Immoos C, Hill MG, Hart PJ, Williams G, Herrmann RG, Valentine JS. 1998. Uclacyanins, stellacyanins, and plantacyanins are distinct subfamilies of phytocyanins: Plant specific monuclear blue copper proteins. *Protein Sci 7*:1915–1929.
Pearson D, Gross EL, David ES. 1996. Electrostatic properties of cytochrome f: Implications for docking with plastocyanin. *Biophys J 71*:64–76.
Qin L, Kostic NM. 1993. Importance of protein rearrangement in the electron-transfer reaction between the physiological partners cytochrome f and plastocyanin. *Biochemistry 32*:6073–6080.
Redinbo MR, Cascio D, Choukair MK, Rice D, Merchant S, Yeates TO. 1993. The 1.5 A crystal structure of plastocyanin from green alga *Chlamydomonas* reinhardtii. *Biochemistry 32*:10560–10567.
Redinbo MR, Yeates TO, Merchant S. 1994. Plastocyanin: Structural and functional analysis. *J Bioenerg Biomembr 26*:49–66.
Richardson DC, Richardson JS. 1992. The kinemage: A tool for scientific communication. *Protein Sci 1*:3–9.
Roberts VA, Freeman HC, Olson AJ, Tainer JA, Getzoff ED. 1991. Electrostatic orientation of the electron-transfer complex between plastocyanin and cytochrome c. *J Biol Chem 266*:13431–13441.
Romero A, De La Cerda B, Varela PF, Navarro JA, Hervas M, De La Rosa MA. 1998. The 2.15 Angstrom crystal structure of a triple mutant plastocyanin from the cyanobacterium Synechocystis sp. PCC 6803. *J Mol Biol 375*: 327–336.
Sali A, Blundell TL. 1993. Comparative protein modeling by satisfaction of spatial restraints. *J Mol Biol 234*:779–815.
Shibata N, Inoue T, Nishio N, Nagano C, Kohzuma T, Onodera K, Yoshizaki F, Sugimura Y, Kai Y. 1999. Novel insight into the copper-ligand geometry in the crystal structure of Ulva pertusa plastocyanin at 1.6 A resolution. Structural basis for regulation of the copper site. *J Biol Chem 274*:4225–4230.
Sigfridsson K, Young S, Hansson O. 1997. Electron transfer between spinach plastocyanin mutants and photosystem I. *Eur J Biochem 245*:805–812.
Soriano GM, Ponamarev MV, Piskorowski RA, Cramer WA. 1998. Identification of the basic residues of cytochrome f responsible for electrostatic docking interactions with plastocyanin in vitro: Relevance to the electron transfer reaction in vivo. *Biochemistry 37*:15120–15128.
Sugawara H, Inoue T, Li C, Gotowda M, Hibino T, Takabe T, Kai Y. 1999. Crystal structures of wild-type and mutant plastocyanins from a higher plant, *Silene*. *J Biochem 125*:899–903.
Sykes AG. 1994. Active-site properties of the blue copper proteins. *Adv Inorg Chem 36*:377.
Thomson JD, Higgins DG, Gibson T. 1994. CLUSTALW: Improving the sensitivity of progressive multiple sequence alignment through sequence weighting, positions-specific gap penalties and weight matrix choice. *Nucleic Acids Res 22*:4673–4680.
Tomic S, Gabdoulline RR, Kojic-Prodic B, Wade RC. 1998a. Classification of auxin plant hormones by interaction property similarity indices. *J Comp-Aided Mol Des 12*:63–79.
Tomic S, Gabdoulline RR, Kojic-Prodic B, Wade RC. 1998b. Classification of auxin related compounds based on similarity of their interaction fields: Extension to a new set of compounds. *Internet J Chem 1*:26.
Ubbink M, Ejdebaeck M, Karlsson BG, Bendall DS. 1998. The structure of the complex of plastocyanin and cytochrome f, determined by paramagnetic NMR and restrained rigid-body molecular dynamics. *Structure 6*:323–335.
Ubbink M, Hunt NI, Hill HA, Canters GW. 1994. Kinetics of the reduction of wild-type and mutant cytochrome c-550 by methylamine dehydrogenase and amicyanin from *Thiobacillus versutus*. *Eur J Biochem 222*:561–571.
Ullmann GM. 1998. Simulation and analysis of docking and molecular dynamics of electron-transfer protein complexes [PhD Thesis]. Free University, Berlin; http://darwin.inf.fu-berlin.de/1998/23/indexe.html.
Ullmann GM, Hauswald M, Jensen A, Kostic NM, Knapp E-W. 1997a. Comparison of the physiologically equivalent proteins cytochrome c6 and plastocyanin on the basis of their electrostatic potentials. Tryptophan 63 in cytochrome c6 may be isofunctional with tyrosine 83 in plastocyanin. *Biochemistry 36*:16187–16196.
Ullmann GM, Knapp E-W, Kostic NM. 1997b. Computational simulation and analysis of the dynamic association between the plastocyanin and cytochrome f. Consequences for the electron transfer reaction. *J Am Chem Soc 119*:42–52.
Van Beeumen J, Van Bun S, Canters GW, Lommen A, Chothia C. 1991. The structural homology of amicyanin from *Thiobacillus versutus* to plant plastocyanins. *J Biol Chem 266*:4869–4877.
van de Kamp M, Silvestrini MC, Brunori M, Van Beeumen J, Hali FC, Canters GW. 1990. Involvement of the hydrophobic patch of azurin in the electron-transfer reactions with cytochrome c551 and nitrite reductase. *Eur J Biochem 194*:109–118.
Van Pouderoyen G, Mazumdar S, Hunt NI, Hill AO, Canters GW. 1994. The introduction of a negative charge into the hydrophobic patch of *Pseudomonas aeruginosa* azurin affects the electron self-exchange rate and the electrochemistry. *Eur J Biochem 222*:583–588.
Vriend G. 1990. WHATIF: A molecular modelling and drug design program. *J Mol Graph 8*:52–56.
Wade RC, Gabdoulline RR, Luedemann SK, Lounnas V. 1998. Electrostatic steering and ionic tethering in enzyme-ligand binding: Insights from simulations. *Proc Natl Acad Sci USA 95*:5942–5949.
Walter RL, Ealick SE, Friedman AM, Blake II RC, Proctor P, Shoham M. 1996. Multiple wavelength anomalous diffraction (MAD) crystal structure of rusticyanin: a highly oxidizing cupredoxins with extreme acid stability. *J Mol Biol 263*:730–751.
Williams PA, Fueloep V, Leung Y-C, Chan C, Moir JWB, Howlett G, Ferguson SJ, Radford SE, Hajdu J. 1995. Pseudospecific docking surfaces on electron transfer proteins as illustrated by pseudoazurin, cytochrome c550 and cytochrome cd1 nitrite reductase. *Nat Struct Biol 2*:975–982.
Xue Y, Okvist M, Young S. 1998. Crystal structure of spinach plastocyanin at 1.7 A resolution. *Protein Sci 7*:2099–2105.
Yamanaka T, Fukumori Y. 1995. Molecular aspects of the electron transfer system which participates in the oxidation of ferrous ion by *Thiobacillus ferrooxidans*. *FEMS Microbiol Rev 17*:401–413.
Young S, Sigfridsson K, Olesen K, Hansson O. 1997. The involvement of the two acidic patches of spinach plastocyanin in the reaction with photosystem I. *Biochim Biophys Acta 1322*:106–114.
Zhu DW, Dahms T, Willis K, Szabo AG, Lee X. 1994. Crystallization and preliminary crystallographic studies of the crystals of the azurin Pseudomonas fluorescens. *Arch Biochem Biophys 308*:469–470.
Zhu Z, Cunane LM, Chen Z, Durley RCE, Mathews FS, Davidson VL. 1998. Molecular basis for interprotein complex-dependent effects on the redox properties of amicyanin. *Biochemistry 37*:17128–17136.